

NUCLEAR HEAVY QUARK PHOTOPRODUCTION IN A SATURATION MODEL

V.P. Gonçalves ¹, M.V.T. Machado ^{1,2}

¹ Instituto de Física e Matemática, Universidade Federal de Pelotas
Caixa Postal 354, CEP 96010-090, Pelotas, RS, Brazil

² High Energy Physics Phenomenology Group, GFPAE, IF-UFRGS
Caixa Postal 15051, CEP 91501-970, Porto Alegre, RS, Brazil

ABSTRACT

We calculate the nuclear inclusive and diffractive cross sections for heavy quark photoproduction within a phenomenological saturation approach. The nuclear cross section is obtained by the extension of the saturation model through Glauber-Gribov formalism. We predict large nuclear heavy quark cross sections at LHC energies.

1 Introduction

During the last years the study of high gluon density effects at high energy (small x) has become an increasingly active subject of research, both from experimental and theoretical points of view. In particular, it has been observed that the ep deep inelastic scattering (DIS) data at low x [1] can be successfully described with the help of the saturation model [2], which incorporates the main characteristics of the high density QCD approaches [3, 4, 5]. In the high energy regime, the growth of parton distributions should saturate, possibly forming a color glass condensate [5] (For a pedagogical presentation see Refs. [6, 7]), which is characterized by a bulk momentum scale Q_s . If the saturation scale is larger than the QCD scale Λ_{QCD} , then this regime can be studied using weak coupling methods. The magnitude of Q_s is associated to the behavior of the gluon distribution at high energies, and some estimates has been obtained. In general, the predictions are $Q_s \sim 1$ GeV at HERA/RHIC and $Q_s \sim 2 - 3$ GeV at LHC [8, 9].

In the phenomenological analysis presented in Refs. [2, 10], the critical line which marks the transition to the saturation regime is smaller than 1 GeV^2 , with larger values predicted only for the next generation of ep colliders. However, deep inelastic scattering on nuclei gives us a new possibility to reach high-density QCD phase without requiring extremely low values of x . The nucleus in this process serves as an amplifier for nonlinear phenomena expected in QCD at small x , obtaining at the accessible energies at HERA and RHIC with an eA collider the parton densities which would be probed only at energies comparable to LHC energies with

an ep collider. In order to understand this expectation and estimate the kinematic region where the high densities effects should be present, we can analyze the behavior of the function $\kappa(x, Q^2) \equiv \frac{3\pi^2\alpha_s}{2Q^2} \frac{xg_A(x, Q^2)}{\pi R_A^2}$, which represents the probability of gluon-gluon interaction inside the parton cascade, and also is denoted the packing factor of partons in a parton cascade [11, 4]. Considering that the condition $\kappa = 1$ specifies the critical line, which separates between the linear (low parton density) regime $\kappa \ll 1$ and the high density regime $\kappa \gg 1$, we can define the saturation momentum scale Q_s given by ¹

$$Q_s^2(x; A) = \frac{3\pi^2\alpha_s}{2} \frac{xg_A(x, Q_s^2(x; A))}{\pi R_A^2}, \quad (1)$$

below which the gluon density reaches its maximum value (saturates). At any value of x there is a value of $Q^2 = Q_s^2(x)$ in which the gluonic density reaches a sufficiently high value that the number of partons stops to rise. This scale depends on the energy of the process [$xg \propto x^{-\lambda}$ ($\lambda \approx 0.3$)] and on the atomic number of the colliding nuclei [$R_A \propto A^{\frac{1}{3}} \rightarrow Q_s^2 \propto A^{\frac{1}{3}}$], with the saturation scale for nuclear targets larger than for nucleon ones. Therefore, we expect that the saturation effects should be manifest in nuclear collisions. Recently, a phenomenological analysis of the multiplicity distributions of produced particles in heavy ion collisions at RHIC, considering the saturation of the nuclear wavefunction, reproduce the experimental data very well [14]. However, the current situation is not unambiguous, since other approaches which do not assume saturation also describe the same set of data. This result motivates more extensive studies of nuclear collisions and, in particular, of electron-nucleus collisions at high energies, where the number of other medium effects is reduced in comparison with AA collisions. Recently, some authors [13, 15, 16] have addressed this subject with particular emphasis in the behavior of the nuclear structure functions (For previous studies see e.g. Refs. [4, 17, 18, 19]), obtaining predictions which agree with the scarce experimental data. Since these models rely on different assumptions, more accurate experimental results for the nuclear structure function in a large kinematical region are necessary to probe the high density dynamics. However, these results compel us to suggest further measurements in electron-nuclei interactions.

Our goal in this paper is to investigate the high energy heavy quark photoproduction on nuclei targets using the saturation hypothesis. The nuclear photoproduction has been recently studied in Ref. [20], obtaining a quite reasonable description of the experimental data, but the specific topic of heavy quark production was not addressed in that analysis. It is important to emphasize that for heavy quark production the predictions are not dependent of the hypothesis for the soft region (e.g. the values of the light quark masses). Here we study the nuclear photoproduction of heavy quarks considering the approach proposed in Ref. [13], which is simpler, gives an equally reasonable agreement with nuclear data as other approaches, and is associated with a model which gives a good description of inclusive and diffractive ep experimental data. A detailed comparison between the distinct saturation approaches for the nuclear case will be presented in a separated publication [21].

¹No exact definition of the saturation scale is known so far. In particular, the Eq. (1) is valid in the double logarithmic approximation. More detailed analysis imply that the enhancement between the nucleon and nuclear cases is smaller than that one predicted in this approximation (See e.g. Refs. [12, 13]).

This paper is organized as follows. In the next section we present a brief review of the saturation model for the nucleon and nuclear case, and the dipole nuclear cross section is analyzed. Section 3 presents our predictions for the energy and atomic number dependence of the heavy quark photoproduction cross section, as well as a detailed analysis of the overlap functions, which allow us to verify what is mean dipole size that contributes for this process. As a by product, in Section 4 the diffractive production of heavy quarks in photonuclear collisions is also considered in the saturation model. Finally, in Section 5 we summarize our conclusions.

2 Nuclear cross sections in a saturation model

In this section we shortly review the main concepts and formulae of the saturation model which is based on the color dipole approach. The latter gives a simple unified picture of inclusive and diffractive processes which provides a large phenomenology on DIS regime. In this approach, the scattering process can be seen in the target rest frame as a succession in time of three factorizable subprocesses: i) the photon fluctuates in a quark-antiquark pair, ii) this color dipole interacts with the target and, iii) the quark pair annihilates in a virtual photon. Using as kinematic variables the γ^*N c.m.s. energy squared $s = W^2 = (p + q)^2$, where p and q are the target and the photon momenta, respectively, the photon virtuality squared $Q^2 = -q^2$ and the Bjorken variable $x = Q^2/(W^2 + Q^2)$, the corresponding total cross section reads as [22, 2]

$$\sigma_{T,L}(x, Q^2) = \int_0^1 dz \int d^2\mathbf{r} |\Psi_{T,L}(z, \mathbf{r}, Q^2)|^2 \sigma_{dip}^{\text{target}}(\tilde{x}, \mathbf{r}^2), \quad (2)$$

where

$$|\Psi_T(z, \mathbf{r}, Q^2)|^2 = \frac{6\alpha_{\text{em}}}{4\pi^2} \sum_f e_f^2 \left\{ [z^2 + (1-z)^2] \varepsilon^2 K_1^2(\varepsilon r) + m_f^2 K_0^2(\varepsilon r) \right\}, \quad (3)$$

$$|\Psi_L(z, \mathbf{r}, Q^2)|^2 = \frac{6\alpha_{\text{em}}}{\pi^2} \sum_f e_f^2 \left\{ Q^2 z^2 (1-z)^2 K_0^2(\varepsilon r) \right\}, \quad (4)$$

are the squared photon wave function for transverse (T) and longitudinal (L) photons, respectively. The variable \mathbf{r} defines the relative transverse separation of the pair (dipole) and z ($1-z$) is the longitudinal momentum fractions of the quark (antiquark). The auxiliary variable $\varepsilon^2 = z(1-z)Q^2 + m_f^2$ depends on the quark mass, m_f . The $K_{0,1}$ are the McDonald functions and the summation is performed over the quark flavors.

For electron-proton interactions, the dipole cross section σ_{dip}^p , describing the dipole-proton interaction is substantially affected by non-perturbative content. There are several phenomenological implementations for this quantity [23]. The main feature of these approaches is to be able to match the soft (low Q^2) and hard (large Q^2) regimes in an unified way. In the present work we follow the quite successful saturation model [2], which interpolates between the small and large dipole configurations, providing color transparency behavior, $\sigma_{dip} \sim \mathbf{r}^2$, as $\mathbf{r} \rightarrow 0$ and constant behavior, $\sigma_{dip} \sim \sigma_0$, at large dipole separations. The parameters of the model have been obtained from an adjustment to small x HERA data. Its parameter-free application to

diffractive DIS has been also quite successful [2] as well as its extension to virtual Compton scattering [24], vector meson production [25] and two-photon collisions [26]. The parameterization for the dipole cross section takes the eikonal-like form,

$$\sigma_{dip}^p(\tilde{x}, \mathbf{r}^2) = \sigma_0 \left[1 - \exp \left(-\frac{Q_s^2(x) \mathbf{r}^2}{4} \right) \right], \quad (5)$$

$$Q_s^2(x) = \left(\frac{x_0}{\tilde{x}} \right)^\lambda \text{ GeV}^2, \quad (6)$$

where the saturation scale Q_s^2 defines the onset of the saturation phenomenon, which depends on energy. The parameters were obtained from a fit to the HERA data producing $\sigma_0 = 23.03$ (29.12) mb, $\lambda = 0.288$ (0.277) and $x_0 = 3.04 \cdot 10^{-4}$ ($0.41 \cdot 10^{-4}$) for a 3-flavor (4-flavor) analysis [2] (See Refs. [10, 16] for improvements of this model). An additional parameter is the effective light quark mass, $m_f = 0.14$ GeV, consistent with the pion mass. It should be noticed that the quark mass plays the role of a regulator for the photoproduction ($Q^2 = 0$) cross section. The light quark mass is one of the non-perturbative inputs in the model. The charm quark mass is considered to be $m_c = 1.5$ GeV. A smooth transition to the photoproduction limit is obtained with a modification of the Bjorken variable as,

$$\tilde{x} = x \left(1 + \frac{4m_f^2}{Q^2} \right) = \frac{Q^2 + 4m_f^2}{W^2}. \quad (7)$$

The saturation model is suitable in the region below $x = 0.01$ and the large x limit needs still a consistent treatment. Making use of the dimensional-cutting rules, here we supplement the dipole cross section, Eq. (5), with a threshold factor $(1-x)^{n_{\text{thres}}}$, taking $n_{\text{thres}} = 5$ for a 3-flavor analysis and $n_{\text{thres}} = 7$ for a 4-flavor one. This procedure ensures consistent description of heavy quark production at the fixed target data [27].

Before going further, some comments on the impact parameter dependence of the saturation model are concerned. The implicit assumption in the approach is that the proton is treated as being homogeneous in the transverse plane. In such case, the impact parameter profile is given by the Heaviside function, $S(b) = \Theta(b_0 - b)$. The profile is considered to be peaked at central impact parameter, namely at $b = 0$. Actually, this procedure is oversimplified and more realistic profiles can be considered. For phenomenological purposes a gaussian or a hard sphere assumption are commonly taken into account. Recently, the impact parameter dipole saturation model [16] was developed, recovering the known Glauber-Mueller dipole cross section. There, distinct shapes for $S(b)$ were considered and their parameters constrained from data on t -dependence of the J/Ψ photoproduction.

Let us discuss the extension of the saturation model for the photon-nucleus interactions. Here, we follow the simple procedure proposed in Ref. [13], which consists of an extension to nuclei, using the Glauber-Gribov picture [28], of the saturation model discussed above, without any new parameter (For similar approaches see e.g. Refs. [4, 29]). There, the nuclear version is obtained replacing the dipole-nucleon cross section in Eq. (2) by the nuclear one,

$$\sigma_{dip}^A(\tilde{x}, \mathbf{r}^2, A) = \int d^2b \, 2 \left\{ 1 - \exp \left[-\frac{1}{2} A T_A(b) \sigma_{dip}^p(\tilde{x}, \mathbf{r}^2) \right] \right\}, \quad (8)$$

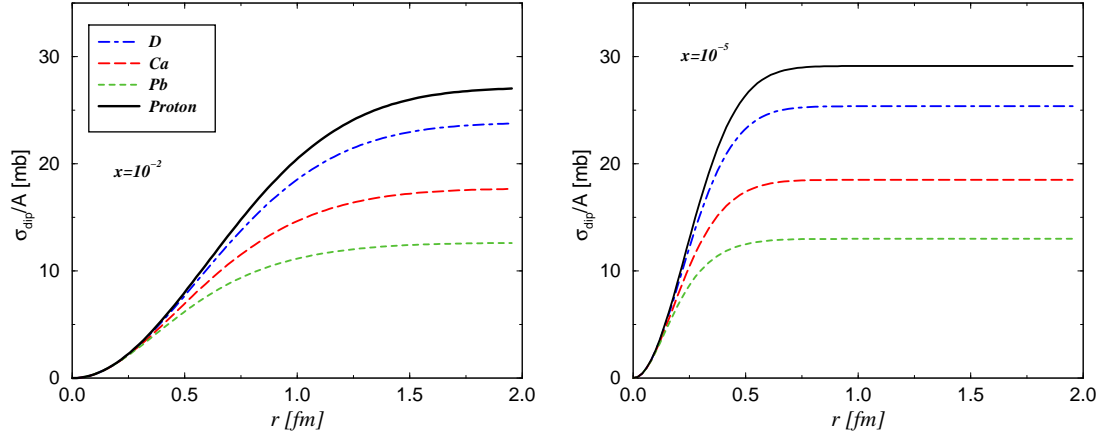


Figure 1: The nuclear dipole cross section as a function of dipole size r for different x values and distinct A , including the proton case. The results are normalized to A .

where b is the impact parameter of the center of the dipole relative to the center of the nucleus and the integrand gives the total dipole-nucleus cross section for a fixed impact parameter. The nuclear profile function is labelled by $T_A(b)$, which will be obtained from a 3-parameter Fermi distribution for the nuclear density [30]. The above equation sums up all the multiple elastic rescattering diagrams of the $q\bar{q}$ pair and is justified for large coherence length, where the transverse separation r of partons in the multiparton Fock state of the photon becomes as good a conserved quantity as the angular momentum, *i. e.* the size of the pair r becomes eigenvalue of the scattering matrix. It is important to emphasize that for very small values of x , other diagrams beyond the multiple Pomeron exchange considered here should contribute (*e.g.* Pomeron loops) and a more general approach for the high density (saturation) regime must be considered. However, we believe that this approach allows us to obtain lower limits of the high density effects in the RHIC and LHC kinematic range. Therefore, at first glance, the region of applicability of this model should be at small values of x , *i.e.* large coherence length, and for not too high values of virtualities, where the implementation of the DGLAP evolution should be required. Therefore, the approach is quite suitable for the analysis of heavy quark photoproduction in the RHIC and LHC kinematical ranges.

In order to investigate the dependence of the nuclear dipole cross section on the dipole size, in Fig. 1 are shown our results for σ_{dip}^A as a function of the dipole size at two fixed values of x . We have select different nuclei $A = D$, Ca and Pb as well the proton case at $x = 10^{-2}$ and $x = 10^{-5}$, with the dipole cross section normalized to A . The behavior on r is the same as the proton case, saturating at large values of r . At small dipole sizes the result is almost independent of A , whereas at large dipole sizes the nuclear suppression is quite substantial and dependent on A . For instance, the reduction in the overall normalization reaches to a factor about 3 for lead in comparison with the nucleon case at small x . This result has sizeable consequences on processes where the large dipole contribution is important, for example in the transversal component of F_2^A and diffractive production of light quarks. For heavy quarks, the situation is different since the corresponding wave functions selects mostly small dipoles configurations, as we will show later on. Having addressed the main concepts and definitions,

in the next section one presents our results for the heavy quark production within the color dipole picture supplemented by the saturation model discussed above. Here, we will focus on photoproduction of charm and bottom in the kinematical range relevant to RHIC and LHC.

3 Nuclear heavy quark photoproduction

In this section we compute the nuclear cross section for the photoproduction of charm and bottom quarks. In this case the nonperturbative input associated with the light quark mass is avoided and we are left with the hard scale given by the heavy quark masses. Here, the following values are taken into account, $m_c = 1.5$ GeV and $m_b = 4.5$ GeV, to be consistent with the previous analysis using the saturation model in the nucleon case. Notice that the use of a different choice implies a distinct overall normalization in the final result.

The cross section for heavy quark photoproduction on nuclei targets is given by

$$\sigma_{tot}^{\gamma A}(W, A) = \int_0^1 dz \int d^2\mathbf{r} |\Psi_T(z, \mathbf{r}, Q^2 = 0)|^2 \sigma_{dip}^A(\tilde{x}, \mathbf{r}^2, A), \quad (9)$$

where the longitudinal contribution is suppressed [See Eq. (4) at $Q^2 = 0$] and $e_{c,b}^2 = 4/9$ and $1/9$, respectively. Accordingly, $m_f = m_{c,b}$ in Eq. (3) and the parameters for the dipole cross section are taken from the 4-flavor analysis. The formula (9) sums up in a compact form all the elastic + inelastic rescattering diagrams of the heavy quark pair with the nucleus.

Before presenting our results for energy dependence of the cross section, we can investigate the mean dipole size dominating the nuclear heavy quark photoproduction. We define the photon-nucleus overlap function which reads as,

$$\mathcal{W}(\tilde{x}, \mathbf{r}, A) = 2\pi r \int dz |\Psi_T(z, \mathbf{r})|^2 \sigma_{dip}^A(\tilde{x}, \mathbf{r}^2, A). \quad (10)$$

In Fig. 2 are shown the overlap function for the charm and bottom production as a function of dipole size. They are computed for lead nucleus and for different x . In the charm case, the distribution is peaked at approximately $r = 0.1$ fm, whereas for the bottom case this value is shifted to $r = 0.05$ fm, which agree with the theoretical expectation that the $q\bar{q}$ pairs have a typical transverse size $\approx 1/m_f$ [29]. Therefore, the main contribution to the cross section comes from the small dipole sizes, i. e. from the perturbative regime. In contrast, for light quarks a broader r distribution is obtained, peaked for large values of the pair separation, implying that nonperturbative contributions cannot be disregarded in that case. For sake of illustration, the transition region between perturbative and nonperturbative regimes ranges at $Q^2 \sim 1/r^2 \simeq 1$ GeV², which means perturbative domain for $r \leq 0.2 - 0.4$ fm. Concerning the high density effects, its value is more sizeable at large dipole configurations (See Fig. 1), meaning that for heavy quark photoproduction we should expect that the associated modifications will be small.

In Fig. 3 are shown the results for the charm and bottom photoproduction cross section as a function of energy for different nuclei, including the proton case. The results present mild growth on W at high energies stemming from the saturation model, whereas the low energy

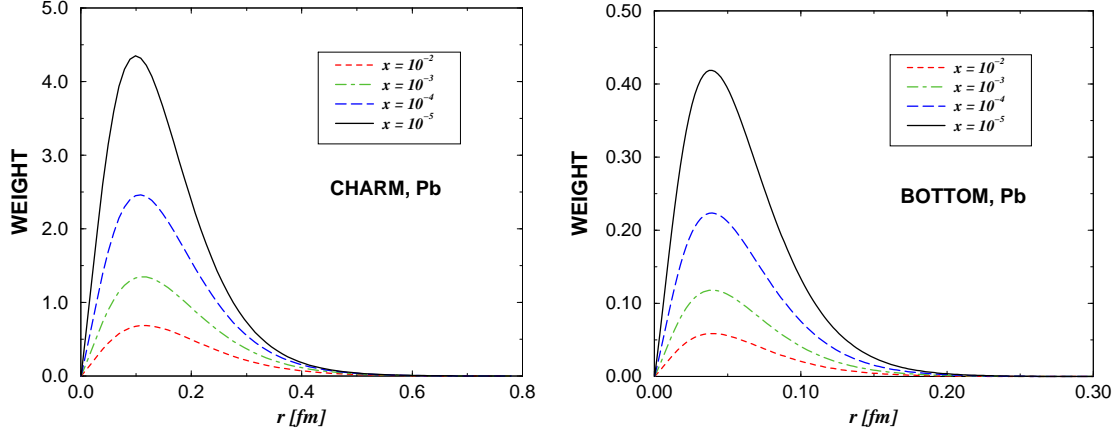


Figure 2: The r dependence of the photon-nucleus overlap function for charm and bottom production, different x and $A = Pb$.

region is consistently described through the threshold factor. For the proton, the experimental data from HERA [31] and fixed target collisions [32] are also included for sake of comparison. The result for charm underestimates data by a factor 2 at $W_{\gamma p} \simeq 200$ GeV, whereas is consistent with the measurements of bottom cross section. Concerning charm production, the measured cross sections present a well known steeper behavior on energy even at electroproduction, suggesting that further resummations in the original saturation model are needed in order to produce the larger growth on energy appearing in the charm measurements. We believe that the better result for bottom happens to be a mismatch between a large uncertainty in the experimental measurement and the lower bottom mass $m_b = 4.5$ GeV considered here. For the nuclear case, we predict that their absolute values are rather large, reaching $\approx 2 \cdot 10^3$ and $\approx 40 \mu b$ for charm and bottom for lead at $W = 10^3$ GeV. It is important to emphasize that our results agree with the predictions obtained for charm photoproduction in the Ref. [33], where the heavy flavor leptonproduction off the nucleus has been addressed considering an approach which resums the fan diagrams of BFKL pomerons, with initial condition for the evolution at $x = 0.01$ given by the Eq. (5). For bottom photoproduction, our results are smaller than Ref. [33]. We believe that our results are reliable, since they are consistent with the simple expectation $\sigma_{\gamma A \rightarrow b\bar{b}X} \approx A \times \sigma_{\gamma p \rightarrow b\bar{b}X}$ for the color transparency regime. A check of the saturation model for the proton case can be found in Ref. [27] and a comparison with other approaches in Ref. [21]. As expected from the discussion in the previous paragraph, the nuclear cross sections can be reasonably approximated by A times the nucleon cross section (Color transparency) [34], since the process is dominated by the scattering of small size dipoles. This result is consistent with the behavior of the dipole cross section presented in Fig. 1, where we have seen that sizeable nuclear effects are only important at large dipole sizes.

Here, an additional issue should be addressed. The dipole-nucleon cross section resums higher twist contributions and also ensures the unitarity requirements, producing a constant value at large r . In order to investigate the effects of this resummation in the dipole-nucleus cross section, we show in Fig. 4 (a) our results for the nuclear photoproduction cross section considering as input the full dipole-nucleon cross section (solid lines), Eq. (5), and only the

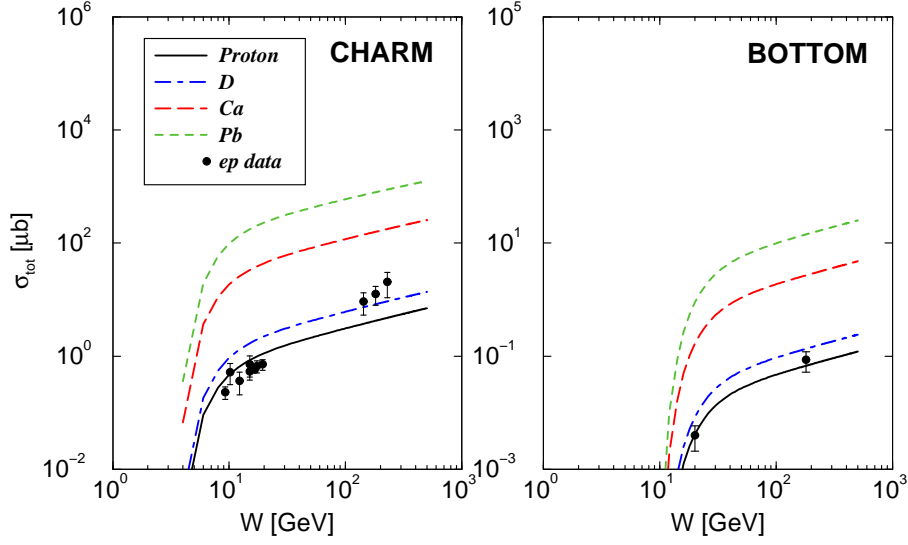


Figure 3: *The total nuclear cross section for charm and bottom photoproduction as a function of cms energy W and distinct nuclei.*

leading term in the expansion of σ_{dip}^p (dot-dashed lines). They were computed for charm quark and considering the calcium and lead nuclei. The effect is almost negligible for light nucleus, whereas it is more sizeable for heavy ones at high energies. This result demonstrate that nuclear heavy quark production is not sensitive to the assumption of a saturated nucleon. In contrast, the behavior of the nuclear structure function depends on the saturation effects at the nucleon level, as shown in Ref. [19].

4 Diffractive photoproduction of heavy quarks

Let us now to compute the diffractive production of heavy quarks. This process was analyzed for ep collisions in Refs. [35, 36, 37]. In terms of the S matrix at a given impact parameter of the collision, $S(b)$, the total and elastic cross sections for the deep inelastic scattering on a nucleus are given by [38]

$$\sigma_{tot} = 2 \int d^2b [1 - S(b)] , \quad (11)$$

$$\sigma_{el} = \int d^2b [1 - S(b)]^2 , \quad (12)$$

which demonstrate how easily the elastic and total cross sections could be obtained from one another. Identifying $1 - S(b)$ with the expression within the brackets in Eq. (8) and considering that diffraction of the photon on the target can be thought as an elastic scattering of each dipole off the nucleus, we obtain that the nuclear diffractive cross section is

$$\sigma_{T,L}^{Diff}(x, Q^2) = \int d^2b \int_0^1 dz \int d^2\mathbf{r} |\Psi_{T,L}(z, \mathbf{r}, Q^2)|^2 \left\{ 1 - \exp \left[-\frac{1}{2} A T_A(b) \sigma_{dip}^p(\tilde{x}, \mathbf{r}^2) \right] \right\}^2 . \quad (13)$$

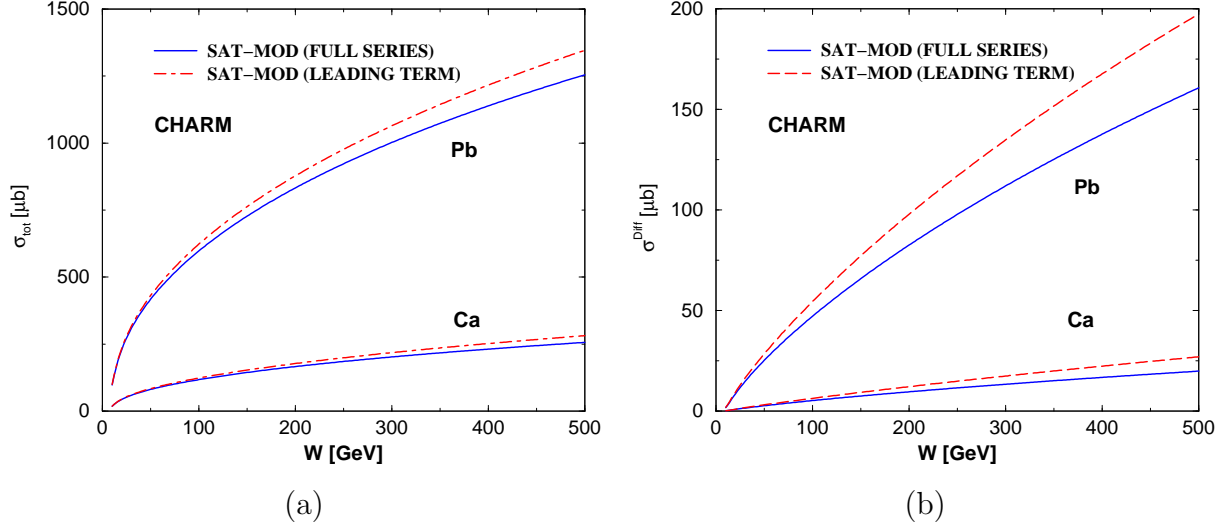


Figure 4: The result for the (a) inclusive and (b) diffractive nuclear charm photoproduction cross section as a function of c.m.s energy for calcium and lead. The solid line corresponds to the full dipole nucleon cross section of the saturation model (full series) and the dot-dashed line is obtained using only the leading term.

For heavy quark photoproduction we have that only the transverse polarization contributes and the wave function is dependent on the heavy quark masses.

Similar analysis of mean size dipole dominance can be made for the diffractive case. Introducing the diffractive overlap function defined by

$$\mathcal{W}^{\text{Dif}}(\tilde{x}, \mathbf{r}, A) = 2\pi r \int d^2b \int dz |\Psi_T(z, \mathbf{r})|^2 \left\{ 1 - \exp \left[-\frac{1}{2} A T_A(b) \sigma_{\text{dip}}^p(\tilde{x}, \mathbf{r}^2) \right] \right\}^2, \quad (14)$$

in Fig. 5 we present our results for the r dependence of this function for different values of x and $A = Pb$. We can see that the distribution is broader and its maximum is shifted to large values of r in comparison with the inclusive case. This result is expected since the diffractive production has a large amount of nonperturbative contributions. However, similarly to the inclusive case, the mean size dipole occur in the perturbative regime, with the large distance still strongly suppressed.

In Fig. 6 the results are shown for the charm and bottom diffractive cross section as a function of energy for different nuclei. The values at high energies are sizeable, reaching to $250 \mu b$ and $0.8 \mu b$ for charm and bottom production, considering lead at $W = 10^3$ GeV. These values are in agreement with a 10% contribution from diffractive scattering to the total cross section observed in photon-nucleon reactions. Concerning the dependence on A , the results present an approximate behavior $\sigma^{\text{Diff}} \simeq A^{4/3}$, as expected for the interaction of small dipoles with the nucleus [39, 40]. We also have checked the diffractive production of heavy quarks for the proton case, with a cross section of order 100 nb at $W = 200$ GeV for diffractive open charm production, being consistent with previous theoretical estimates [37]. There, it was found a value of 60 nb at the same energy in the photoproduction case. A more detailed analysis for the proton case should be addressed elsewhere.

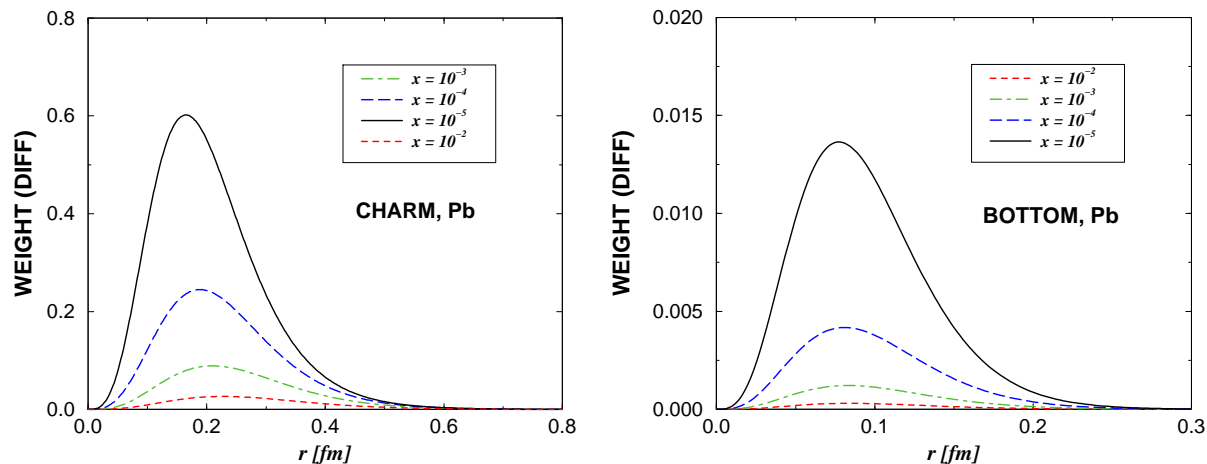


Figure 5: *The r dependence of the diffractive photon-nucleus overlap function for charm and bottom production, different x and $A = Pb$.*

Finally, in Fig. 4 (b) we analyze the dependence of the diffractive nuclear cross section in considering or not a saturated proton, namely saturation effects in the nucleon level. We can see that while for a light nuclei the cross section is not sensitive to the assumption of a saturated nucleon, for a heavy nuclei the result differs by about 20%. Therefore, the analysis of the diffractive cross section can be useful to constraint the nucleon dynamics.

5 Summary and Conclusions

In this paper we have calculated the nuclear inclusive and diffractive cross sections for heavy quark photoproduction within a phenomenological saturation model. In such model the nuclear cross section is obtained through the Glauber-Gribov formalism. Since it describes reasonably the experimental data for the nuclear structure function, we are confident in extending this model for the nuclear heavy quark photoproduction case. Moreover, it is simple and relies on a model which gives a good description of inclusive and diffractive ep experimental data. This model should be valid until the full non-linear evolution effects become important, which implies the consideration of the Pomeron loops beyond the multiple scattering on single nucleons estimated in the present framework. We have verified that the main contribution of the high density effects occur for large pair separation, while for dipoles of small size they are almost negligible. We have investigated the mean dipole size dominance and have verified that the heavy quark cross section is dominated by small dipole configuration, in contrast to the light quark case. Consequently, we have that the nuclear heavy quark production is not strongly modified by the high density effects. We predict absolute values for the cross section rather large, being about 2 mb and 0.04 mb for charm and bottom, respectively, for lead and $W = 1$ TeV. These values are similar to those resulting from the resummation of the fan diagrams of BFKL pomerons. Furthermore, we have computed the diffractive nuclear photoproduction of heavy quarks. This quantity is more sensitive to the nonperturbative sector, corresponding

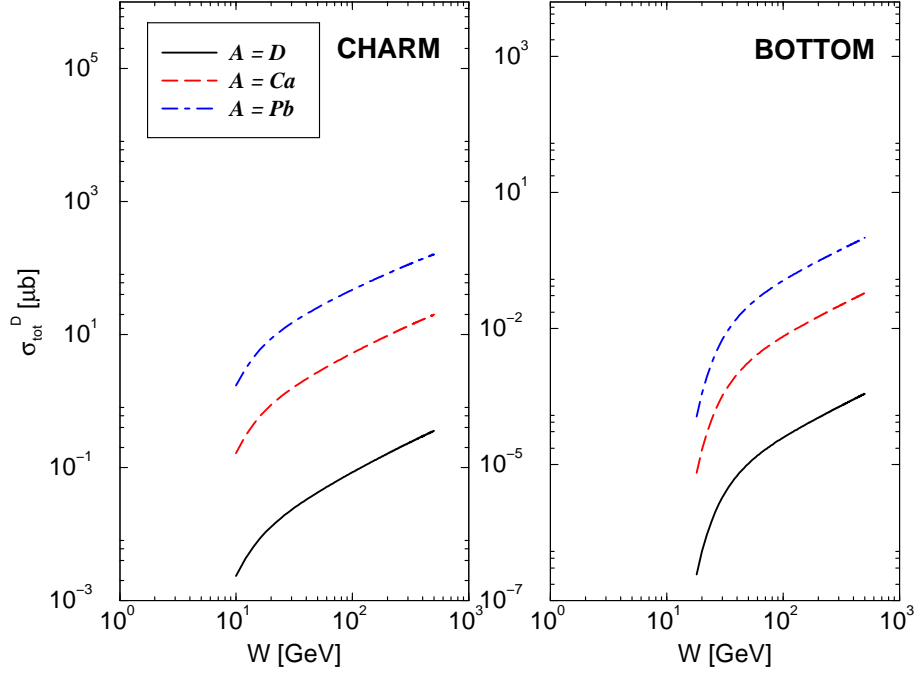


Figure 6: *The diffractive nuclear cross section for charm and bottom photoproduction as a function of c.m.s. energy W and for distinct nuclei.*

to a larger dipole sizes. This means that the cross section is dominated by larger dipole configurations than in the inclusive case. The results take values about $250 \mu b$ and $0.8 \mu b$ for charm and bottom for lead at $W = 1$ TeV. Concerning the A -dependence, we have found a behavior proportional to A and $A^{4/3}$ for the inclusive and diffractive cross sections, respectively, in agreement with theoretical expectations associated with the color transparency regime.

Acknowledgments

M.V.T.M. thanks the support of the High Energy Physics Phenomenology Group at the Institute of Physics, GFPAE IF-UFRGS, Porto Alegre. This work was partially financed by the Brazilian funding agencies CNPq and FAPERGS.

References

- [1] M. Klein, Int. J. Mod. Phys. A **15S1**, 467 (2000).
- [2] K. Golec-Biernat, M. Wüsthoff, Phys. Rev. D **59**, 014017 (1999); Phys. Rev. D **60**, 114023 (1999).

- [3] Ia. Balitsky, Nucl. Phys. B **463**, 99 (1996); Yu. Kovchegov, Phys. Rev. D **60**, 034008 (1999).
- [4] A. L. Ayala, M. B. Gay Ducati, E. M. Levin, Nucl. Phys. **B493**, 305 (1997).
- [5] E. Iancu, A. Leonidov, L. McLerran, Nucl. Phys. A **692**, 583 (2001); E. Ferreiro, E. Iancu, A. Leonidov, L. McLerran, Nucl. Phys. A **703**, 489 (2002).
- [6] E. Iancu, A. Leonidov, L. McLerran, ePrint Archive: [hep-ph/0202270].
- [7] E. Iancu, R. Venugopalan, ePrint Archive: [hep-ph/0303204].
- [8] M. Gyulassy, L. McLerran, Phys. Rev. C **56**, 2219 (1997).
- [9] V. P. Gonçalves, Phys. Lett. B **495**, 303 (2000).
- [10] J. Bartels, K. Golec-Biernat, H. Kowalski, Phys. Rev. D **66**, 014001 (2002).
- [11] L. V. Gribov, E. M. Levin and M. G. Ryskin, Phys. Rept. **100**, 1 (1983).
- [12] E. Levin, K. Tuchin, Nucl. Phys. A **693**, 787 (2001); E. Levin, M. Lublinsky, Nucl. Phys. A **696**, 833 (2001).
- [13] N. Armesto, Eur. Phys. J. C **26**, 35 (2002).
- [14] D. Kharzeev, M. Nardi, Phys. Lett. B **507**, 121 (2001); D. Kharzeev, E. Levin, Phys. Lett. B **523**, 79 (2001).
- [15] N. Armesto *et al.*, ePrint Archive: [hep-ph/0304119].
- [16] H. Kowalski, D. Teaney, ePrint Archive: [hep-ph/0304189].
- [17] K. J. Eskola, J. W. Qiu, X. N. Wang, Phys. Rev. Lett. **72**, 36 (1994).
- [18] Z. Huang, H. J. Lu, I. Sarcevic, Nucl. Phys. A **637**, 79 (1998).
- [19] M. B. Gay Ducati, V. P. Gonçalves, Phys. Rev. C **60**, 058201 (1999).
- [20] J. Bartels *et al.*, ePrint Archive: [hep-ph/0304166].
- [21] V. P. Gonçalves, M. V. T. Machado, ePrint Archive: [hep-ph/0307129].
- [22] N. N. Nikolaev, B. G. Zakharov, Phys. Lett. B **332**, 184 (1994); Z. Phys. C **64**, 631 (1994).
- [23] J.R. Forshaw, G. Kerley, G. Shaw, Phys. Rev. D **60**, 074012 (1999);
M. McDermott, L. Frankfurt, V. Guzey, M. Strikman, Eur.Phys.J. C **16**, 641 (2000);
E. Gotsman *et al.*, J. Phys. G **27**, 2297 (2001).
A. Donnachie, H.G. Dosch, Phys. Rev. D **65** 014019 (2002);
M.B. Gay Ducati, M.V.T. Machado, Phys. Rev. D **65**, 114019 (2002);
M.A. Betemps, M.B. Gay Ducati, M.V.T. Machado, Phys. Rev. D **66**, 014018 (2002).

- [24] L. Favart, M. V. T. Machado, Eur. Phys. J. C (in press), ePrint Archive: [hep-ph/0302079].
- [25] A. C. Caldwell, M. S. Soares, Nucl. Phys. A **696**, 125 (2001).
- [26] N. Timneanu, J. Kwiecinski, L. Motyka, Eur. Phys. J. C **23**, 513 (2002).
- [27] C. Brenner Mariotto, M. B. Gay Ducati, M. V. T. Machado, Phys. Rev. D **66**, 114013 (2002).
- [28] V. N. Gribov, Sov. Phys. JETP **29**, 483 (1969); Sov. Phys. JETP **30**, 709 (1970).
- [29] N. N. Nikolaev, B. G. Zakharov, Phys. Lett. B **260**, 414 (1991); Z. Phys. C **49**, 607 (1991).
- [30] C. W. De Jager, H. De Vries, C. De Vries, Atom. Data Nucl. Data Tabl. **14**, 479 (1974).
- [31] S. Aid *et al.* (H1 collaboration), Nucl. Phys. **B472**, 32 (1996);
C. Adloff *et al.* (H1 collaboration), Phys. Lett. B **467**, 156 (1999).
- [32] M.S. Atiya *et al.*, Phys. Rev. Lett. **43**, 414 (1979);
D. Aston *et al.* (WA4 collaboration), Phys. Lett. B **94**, 113 (1980);
J.J. Aubert *et al.* (EMC collaboration), Nucl. Phys. **B213**, 31 (1983);
K. Abe *et al.* (SHFP collaboration), Phys. Rev. Lett. **51**, 156 (1983);
K. Abe *et al.* (SHFP collaboration), Phys. Rev. D **33**, 1 (1986);
M.I. Adamovich, Phys. Lett. B **187**, 437 (1987);
J.C. Anjos *et al.* (The Tagged Photon Spectrometer collaboration), Phys. Rev. Lett. **65**, 2503 (1990);
J.J. Aubert *et al.* [European Muon Collaboration], Phys. Lett. B **106**, 419 (1981).
- [33] N. Armesto, M. A. Braun, Eur. Phys. J. C **22**, 351 (2001).
- [34] S. J. Brodsky, A. H. Mueller, Phys. Lett. B **206**, 685 (1988).
- [35] M. Genovese, N. N. Nikolaev, B. G. Zakharov, Phys. Lett. B **378**, 347 (1996).
- [36] E. M. Levin, A. D. Martin, M. G. Ryskin, T. Teubner, Z. Phys. C **74**, 671 (1997).
- [37] M. Diehl, Eur. Phys. J. C **1**, 293 (1998).
- [38] A. H. Mueller, Eur. Phys. J. A **1**, 19 (1998).
- [39] N. N. Nikolaev, B. G. Zakharov, V. R. Zoller, Z. Phys. A **351**, 435 (1995).
- [40] M. Arneodo *et al.*, in Proceedings of the workshop on Future Physics at HERA, Eds.: G. Ingelman, A. De Roeck, R. Klanner, vol. 2, pp. 887-926 (1996).